Dynamical Nonlinear Inversion of the Surface Photovoltage at Si(100)

Friedrich Roth,[1,2,*] Johannes Mahl,[3] Mario Borgwardt,[3] Lukas Wenthaus,[4] Felix Brausse,[3,‡] Valentin Garbe,[5] Oliver Gessner,[3] and Wolfgang Eberhardt[4,†]

[1]*Institute of Experimental Physics, TU Bergakademie Freiberg, 09599 Freiberg, Germany*
[2]*Center for Efficient High Temperature Processes and Materials Conversion (ZeHS), TU Bergakademie Freiberg, 09599 Freiberg, Germany*
[3]*Chemical Sciences Division, Lawrence Berkeley National Laboratory, Berkeley, California 94720, USA*
[4]*Center Center for Free-Electron Laser Science CFEL, Deutsches Elektronen-Synchrotron DESY, 22607 Hamburg, Germany*
[5]*Institute of Applied Physics, TU Bergakademie Freiberg, 09599 Freiberg, Germany*

(Received 15 September 2022; revised 2 January 2024; accepted 14 February 2024; published 3 April 2024)

A surface photovoltage (SPV) is observed whenever a doped semiconductor with non-negligible band bending is illuminated by light and charge carriers are excited across the band gap. The sign of the SPV depends on the nature of the doping, the amplitude of the SPV increases with the fluence of the light illumination up to a saturation value, which is determined by the doping concentration. We have investigated Si(100) samples with well-characterized doping levels over a wide range of illumination fluences. Surprisingly, the sign of the SPV upon illumination with 532 nm photons reverses for some *p*-doping concentrations at high fluences. This is a new effect associated with a crossover between electronic excitations in the bulk and at the surface of the semiconductor.

DOI: 10.1103/PhysRevLett.132.146201

Charge carrier excitation, transport, and recombination are important for the design and performance of semiconductor devices and/or photovoltaic cells. Yet, especially on femtosecond (fs) and picosecond (ps) timescales, these charge carrier dynamics are still not completely understood. New characterization tools have recently been developed at synchrotron radiation sources and x-ray free electron lasers (XFELs), allowing the investigation of these ultrafast dynamical processes with, for example, time-resolved x-ray photoemission spectroscopy (tr-XPS). Here, we present such a study for one of the most elementary semiconductors: clean Si(100). We observe dramatic and unexpected variations of the SPV, including a sign change, when investigating Si samples under a wide range of illumination levels for both *p*- and *n*-doped samples.

Because of the technological impact, the electronic structure investigation of Si has attracted a lot of attention as early as the basic concepts of the band structure of solids, surface states, and dopant-induced impurity levels had been developed. Initially, optical spectroscopy revealed the band gap energy values as well as the location of impurity states. The surface electronic structure was at least partially revealed by measuring the work function of the sample as soon as clean surfaces could be prepared and observed in high and ultrahigh vacuum environments [1]. Early approaches to measuring SPVs are described extensively in various reviews [2–4]. As early as 1971, not only the bulk interband transitions but also specific optical excitations of electrons at the surface were identified to cause changes in the observed SPV under sub-band gap illumination [3].

In a simplified view, the Fermi Level in the bulk is determined by the doping level, whereas at the surface it is located between the occupied and unoccupied surface states, almost independent from the bulk doping levels. For $\mathrm{Si}(100)(2\times1)$, which is studied here, the surface bandgap amounts to 800 meV and the midgap position is 250 meV above the surface valence band edge, as determined by angle-resolved photoemission and inverse photoemission [5–7]. Accordingly, the *n*-type (*p*-type) semiconductor displays upward (downward) band bending near the surface. Upon illumination, charge carriers are excited across the band gap and these charges are diffusing until the bands are flattened out. This results in a shift to smaller binding energies for all electronic states in *p*-doped samples, whereas for *n*-doped samples the shift is in the opposite direction to larger binding energies.

While SPV spectroscopy is a well-established tool for the characterization of semiconductor electronic structures, systematic studies involving a large variety of doping levels, types, and illumination fluences are rare. Here, we perform such a study on $\mathrm{Si}(100)(2\times1)$ using picosecond tr-XPS. The measurements reveal partly complex variations of SPV effects, depending on the exact sample conditions and experimental parameters. Significant changes in the dynamic trends occur and even a surprising reversal of the SPV sign with increasing fluence for some p-doped samples is observed. The results are interpreted

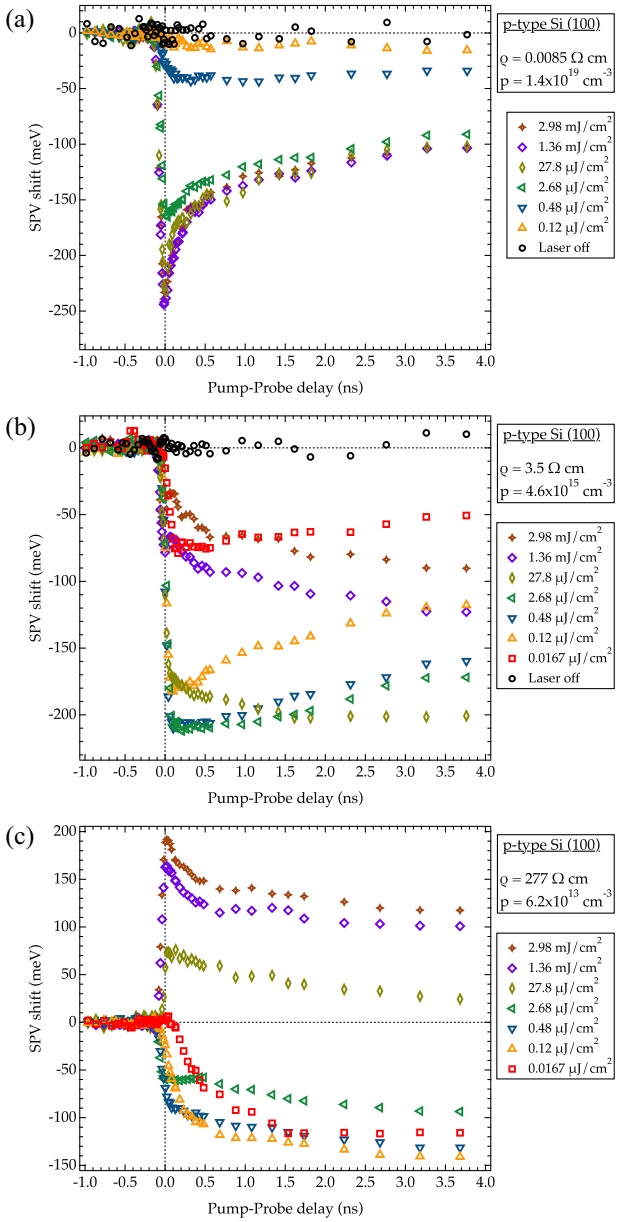

FIG. 1. Observed SPV shifts for clean p-doped Si(100) for three different doping levels [high (a), intermediate (b), and low (c)] and a range of laser fluences as indicated. Positive shifts correspond to higher binding energies after laser excitation compared to the ground-state spectra.

within the picture of a competition between bulk and surface excitations, whereby the latter dominates at higher fluences.

The experimental setup has previously been described [8–11], details specific to the study presented here are given in the Supplemental Material [12].

Figure 1 shows the observed SPV of clean Si(100) for various p-doped samples with different doping concentrations and several laser illumination fluences, as determined by picosecond time-resolved high-resolution Si $2p$ core level photoemission. Positive (negative) SPV shifts correspond to larger (smaller) binding energies of the Si $2p$ core level relative to the nonilluminated sample. For highly p-doped Si ($p = 1.4 \times 10^{19}$ cm^{-3}), [Fig. 1(a)], we observe a negative SPV shift, as expected for this kind of doping. We distinguish two different temporal regions in these spectra. The long-term behavior, i.e., the values of the SPV ~3 ns after excitation or later, and the short-term behavior up to ~1 ns. With increasing laser fluences, the plateau of the long-term SPV shift initially increases roughly linearly with the incident fluence, but then saturates for fluences beyond ~3 μJ/cm^2. The short-term SPV dynamics also change with fluence. While for fluences below ~1 μJ/cm^2 the SPV rises within ~200 ps and then remains essentially constant, at higher fluences the SPV exhibits an "overshoot," which rises more rapidly within the instrument response time (~70 ps) and then decays partially within ~1 ns to a level that then remains almost constant for many ns.

For low p-doped samples ($p = 6.2 \times 10^{13}$ cm^{-3}) [Fig. 1(c)] the behavior changes completely. For low laser fluences, the SPV shift is again negative up to a long-term plateau level of approximately −140 meV as expected. However, when the laser fluence is increased from 0.48 (blue triangles) to 2.68 μJ/cm^2 (green triangles), the magnitude of the SPV shift actually decreases and, for higher fluences, it even changes sign to positive values (higher binding energies). For the highest fluences, a rapid SPV overshoot is observed for the first 500 ps, similar to the results for highly p-doped samples [see Fig. 1(a)] but with an opposite sign. Such an inversion of the SPV with increase in the strength of the illumination has never been observed before. For intermediate p-doping levels of $p = 4.6 \times 10^{15}$ cm^{-3} [Fig. 1(b)] we see yet a different behavior. For low laser fluences up to ~30 μJ/cm^2, a SPV shift is observed that first increases with laser fluence, then saturates at approximately −200 mV, with the saturation accompanied by a change in the dynamic trends. This SPV is slightly larger than expected for this dopant concentration. However, upon increasing the laser fluence to a value of 1.36 mJ/cm^2 (purple diamonds), the SPV actually decreases, in particular, for the first few hundred ps after photoexcitation. For an even higher fluence of 2.98 mJ/cm^2, the SPV decreases even further, but it does not change sign as observed for the sample with the lowest level of p doping.

The nonlinear SPV behavior under illumination and its dependence on doping levels are completely new. Most previous studies did not report exact doping levels. The observation that the SPV changes sign with increased strength of the illumination is quite surprising and has not been previously observed [13–18]. As far as studies under different illumination strengths were reported, the results generally showed an increase of the SPV up to a certain level of saturation [14–16,19]. Concerning a different sample property, Mauerer *et al.* [18] report a decrease of

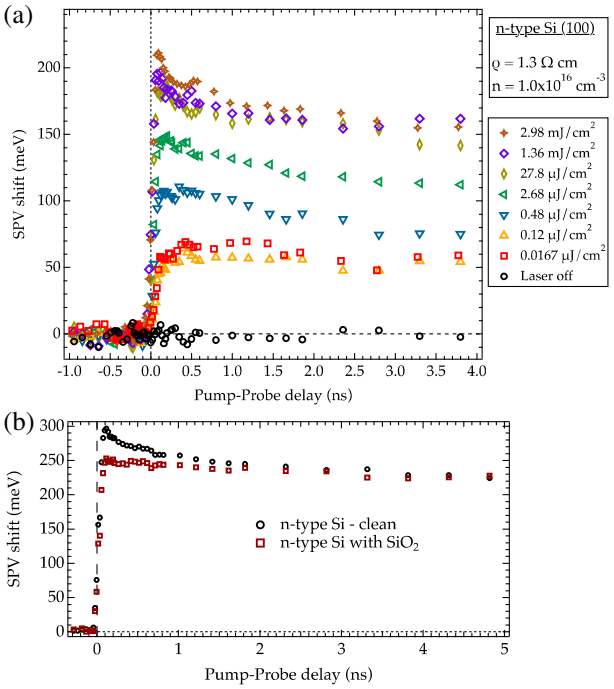

FIG. 2. Observed SPV shift for n-doped Si(100) as a function of the fluence of the optical laser for high doping level (a), and the comparison between the SPV shift of a clean and oxidized n-doped wafer (b) measured with a fluence of 3.38 $\mathrm{mJ/cm^2}$.

the SHG signal with increasing laser power for the Si (111) surface, which the authors associate with the population of unoccupied surface states. While the SPV was not measured in this study, we see that these results are significant in the context of our observations reported here also.

Before we enter into a discussion and provide an explanation of this surprising SPV behavior, we first present results for a clean and an oxidized n-doped wafer. For the clean sample [Fig. 2(a)], we observe a SPV shift to larger binding energy (positive values) as expected from the simple SPV model introduced above. With increasing fluence, the long-term plateau of the SPV dynamics reaches a saturation value of 160 meV, and additionally, an overshoot develops at the onset. We have also investigated other n-doped samples with different doping levels, but all of these showed qualitatively the same behavior as in Fig. 2(a) (cf. Fig. S1 in the Supplemental Material [12]). For n-doped samples, the only change in the SPV with doping is that its maximum extent decreases with decreasing levels of doping, as expected, but no amplitude trend or sign inversions are observed when varying the illumination fluence, as in the p-doped samples.

Comparison between the SPV of a clean and an oxidized n-doped Si(100) wafer (doping concentration $n = 1 \times 10^{16}$ $\mathrm{cm^{-3}}$) at the same laser fluence [cf. Fig. 2(b)] shows that, for the oxidized sample, the overshoot at short timescales is missing. This is a strong indication that this overshoot at the onset is associated with the excitation and population of electronic surface states. The difference in the absolute values of the SPV in Figs. 2(a) and 2(b) is tentatively assigned to a small shift of the surface Fermi level position within the band gap due to surface defects. The surface Fermi level depends on the density of defects and, accordingly, can change with each cleaning procedure.

In order to explain our observations, we have to have a look at the basics of the surface photovoltage effect and specifically include surface excitations as shown in Fig. 3. Most recent discussions of the SPV disregarded this latter term and focused exclusively on bulk interband excitations. The ground state situation without illumination is depicted in Fig. 3(a) for p-doped Si(100) (upper panel) and n-doped Si(100) (lower panel). In the bulk of the semiconductor, the Fermi level is located near the valence or conduction band edges, depending on the type and concentration of the dopants. The Fermi level at the surface, on the other hand, is located closer to the middle of the "surface band gap" as determined by the location and occupation of the surface states. These are indicated by rectangles in Fig. 3. Their energy positions are shown according to the reported values for the $\mathrm{Si}(100)(2 \times 1)$ surface [15]. Blue-filled areas within the rectangles indicate electron populations. The difference of the Fermi level position in the bulk and at the surface causes band bending, effectively establishing a space charge region to screen the surface charges. According to Poisson's equation, the bulk Fermi potential is reached at a depth where the surface charges responsible for the potential at the surface are screened by the doping charges. The depth of the space charge region defines the region of the band bending and scales inversely with the square root of the dopant concentration. This depth corresponds to values between 2 and 2000 nm for dopant levels around 10^{20} and 10^{14} $\mathrm{cm^{-3}}$, respectively [1,20]. We observe the SPV by using tr-XPS to monitor the binding energy of the Si $2p$ core levels. In general, the escape depth of the electrons is significantly shorter than the depth of the band-bending region, such that XPS photoemission essentially reflects the band position at the surface.

Illumination of the sample by photons exceeding the band gap energy will cause the creation of electron-hole pairs. The different charge carriers are separated in the electric field between bulk and surface, which also creates the band bending. While one type of carrier diffuses into the bulk, the other remains in the surface region and screens the surface charges, which leads to a dynamic flattening of the bands as indicated in Fig. 3(b). Once the bands are flat, there is no driving field and charge migration and separation will stop. In this flat band condition, the position of the surface Fermi level relative to the band edges is the same as in the bulk. This is the general model used to explain the SPV.

So far, we have only considered excitations in the bulk due to interband transitions. If we (hypothetically) only

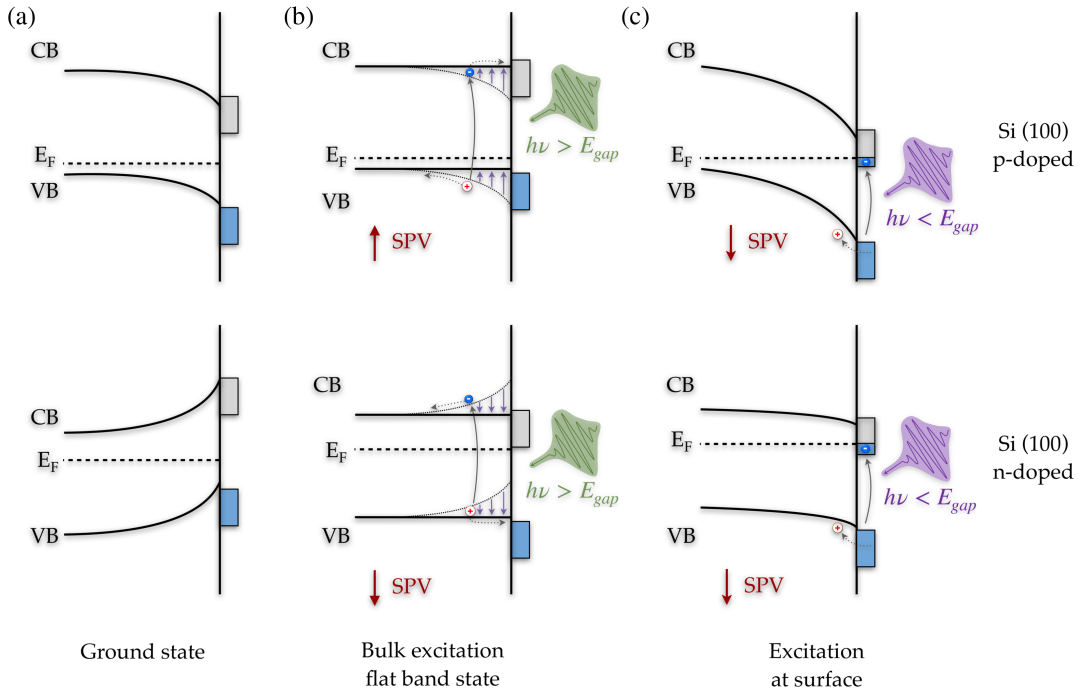

FIG. 3. Schematic diagrams showing the energy levels near the surface of a clean semiconductor: band bending at the surface of Si(100) in the ground state (a) and under illumination and photon absorption in the bulk (b) for *p* doping (upper panel) and *n* doping (lower panel). In (c) the SPV shift is shown for surface excitations only.

consider excitations at the surface due to transitions between occupied and unoccupied surface states, we arrive at a situation as indicated in Fig. 3(c). Because of the dispersion of the surface states, at certain points in *k* space, away from the center of the surface Brillouin zone, direct transitions between occupied and unoccupied surface states are directly excited by the light of 532 nm wavelength in our experiment [5–7]. Whenever the population of the surface states changes, the Fermi level position at the surface follows, which in turn affects the band bending and leads to the observation of a shift of the levels.

This may be referred to as the surface contribution to the SPV. Concerning the population of the surface states, for Si(100), because of the energetic overlap of the occupied surface states with the bulk bands, the holes will quickly diffuse into the bulk, while the surface state electrons remain trapped by the surface barrier. This then leads to a situation as depicted in Fig. 3(c). It creates a completely different situation as far as the SPV dependency on doping is concerned. For *n*-doped samples, the SPV is only marginally enhanced compared to the flat band state, while for *p*-doped samples the SPV shift reverses in sign to higher binding energies as indicated in the upper part of Fig. 3(c). This is exactly what we observe for the low *p*-doped sample.

As our illumination photon energy of 2.33 eV is above the band gap of silicon, we see a mixture and competition between dynamics induced by bulk and surface excitations. For low fluences bulk excitations dominate. All of the incoming photons are eventually absorbed creating bulk interband transitions and we observe the conventional SPV. As far as bulk interband transitions are concerned, the SPV will essentially saturate as soon as flat band conditions are reached.

As the fluence is increased, a larger number of photons is absorbed in total, but also specifically at the surface. That means that in absolute terms a significant fraction of the surface state population will get excited. For high fluences the excitations involving a significant change in the occupation of the surface states become a dominant factor. Mauerer *et al.* [18] report for 800 nm excitation at a fluence of 10 mJ/cm^2 that the population of originally unoccupied surface states on Si (111) reaches saturation at a level exceeding 50% of occupation. At 532 nm the cross-section is significantly larger so this saturation should be reached at lower laser fluences.

The excitation does not even have to proceed directly between occupied and unoccupied surface states but may also involve bandgap excitation and relaxation into a surface excitation as reported by Weinelt *et al.* [15]. Once these surface states are partially occupied, the Fermi level at the surface moves from near midgap into the energy region of the originally empty surface states, which corresponds to a binding energy shift of approximately 400 meV to larger binding energies. This is sufficient to reverse the sign of the SPV for *p*-doped samples, as observed in the experiment in the weak doping regime. On Si(100) we also encounter the particular

situation that the lower energy surface band states are completely degenerate with the valence band, while the upper (unoccupied) surface band is located in the bulk bandgap. Accordingly, holes in the lower surface band states readily diffuse into the bulk, and bulk excited electrons may relax into the upper surface band states, but electrons excited at the surface cannot escape into the bulk because of the surface barrier.

As far as the dynamics of the SPV is concerned, we propose that direct surface excitations cause a faster transient and a shorter risetime of the potential change, whereas bulk excitations involve the diffusion of carriers and, accordingly, are a bit slower. The initial overshoot is associated with direct surface excitations and accordingly the transient is sharper, which explains the differences in risetime noted in the discussions of the results shown in Fig. 1.

Thus, we conclude that the effects we observe result from a competition between excitations in the bulk and at the surface. The proposed model also qualitatively explains the differences we observe for p-doped samples with different doping concentrations (see Fig. 1). For low dopant concentrations, the depletion region reaches deep into the bulk and the electric field driving diffusion of charges between the surface and the bulk is fairly small. Accordingly, what we see is largely dominated by the processes at the surface as soon as the excitation level at the surface is significant. For low p-doped samples, any diffusion of charges between the surface and the bulk is rather limited. For the intermediate p-doping concentration, the competition between bulk and surface excitations is most clearly visible. At high fluences, when surface excitations become significant, we do observe a surface SPV component. This, however, is not sufficiently strong to overcome the effect of bulk excitations. For high p doping we see mostly bulk behavior. The enhancement of the overshoot at the highest fluences is tentatively associated with additional depletion of originally populated surface states, which quickly diffuse into the bulk.

We close the discussion by considering the potential impact of the so-called Dember effect on the reported results [21]. Electrons and holes in Si—as in many other semiconductors—have different mobilities with electron mobilities exceeding those of holes by a factor of ≈3–3.5. The resulting differences in diffusion behavior result in internal fields and SPV contributions [21]. Quantitative estimates for Dember voltages and their dynamic trends under our experimental conditions are challenging since currently available software packages (e.g., for photovoltaic applications) do not cover the relevant range of excitation densities. A rough estimate based on Eq. 1.57 in Ref. [21] places the Dember voltages for the p-doped samples with the highest, medium, and lowest doping levels at approximately 20, 130, and 200 mV, respectively, for the maximum laser fluence of 2.98 mJ/cm^2. Corresponding SPV shifts would be toward positive SPV values, for both p and n doping. For p-doped samples, this would be in the direction of the unexpected inversion and, therefore, could principally contribute to the observed effects. The relatively slow relaxation times of the inverted SPV transients, however, which extend out to microseconds (see Fig. S2 [12]), make it unlikely that the Dember effect is the predominant mechanism. For Si at the high excitation densities associated with the inverted SPV region, Dember voltage decay timescales are expected to be dominated by internal recombination through three-body Auger-like processes [22,23]. Auger lifetimes for the two highest laser fluences of 1.36 and 2.98 mJ/cm^2, corresponding to estimated excitation densities of $\sim 2 \times 10^{19}$ to $\sim 4 \times 10^{19}$ cm^3, are expected to range from ∼2.4 ns to ∼600 ps [22]. These lifetimes are orders of magnitude shorter than the ones observed in the experiment. For comparison, radiative lifetimes of excited carriers in Si are even longer (ms range), due to the indirect band gap [22]. Thus, the Dember effect, while possibly contributing to the initial sample response, is unlikely to dominate the long-lived SPV inversion on many nanosecond to microsecond timescales.

In summary, something as simple and established as the SPV effect actually exhibits a complex nonlinear behavior when the dependence on doping and excitation fluence is studied. Our detailed experimental data reveal a competition between bulk and surface excitations, whereby at higher illumination the change in the population of surface levels becomes the dominant factor. Qualitatively we can explain these observations, but a detailed theoretical modeling would be very welcome to support our interpretation quantitatively.

W. E. wants to specifically thank U. Höfer and T. Tiedje for stimulating discussions. This work was supported within the program "Structure of Matter" of the Helmholtz Association and by the BMBF (Grant No. 05K22OF2 within ErUM-Pro). J. M., M. B., F. B., and O. G. were supported by the Atomic, Molecular, and Optical Sciences Program of the U.S. Department of Energy, Office of Science, Office of Basic Energy Sciences, Chemical Sciences, Geosciences, and Biosciences Division, through Contract No. DE-AC02-05CH11231. F. R. acknowledges financial support by the VI 419 of the Helmholtz Association. M. B. acknowledges support by the Alexander von Humboldt foundation. We would like to thank the staff at the ALS, especially Monika Blum, for their excellent support during the experiment. This research used resources of the Advanced Light Source, which is a DOE Office of Science User Facility under Contract No. DE-AC02-05CH11231.

*Corresponding author: friedrich.roth@physik.tu-freiberg.de
†Corresponding author: wolfgang.eberhardt@cfel.de
‡Present address: European XFEL GmbH, Holzkoppel 4, 22869 Schenefeld, Germany.

[1] F. G. Allen and G. W. Gobeli, Work function, photoelectric threshold, and surface states of atomically clean silicon, Phys. Rev. **127**, 150 (1962).

[2] L. Kronik and Y. Shapira, Surface photovoltage phenomena: Theory, experiment, and applications, Surf. Sci. Rep. **37**, 1 (1999).

[3] C. L. Balestra, J. Łagowski, and H. C. Gatos, Determination of surface state energy positions by surface photovoltage spectrometry: CdS, Surf. Sci. **26**, 317 (1971).

[4] Z. Zhang and J. T. Yates, Band bending in semiconductors: Chemical and physical consequences at surfaces and interfaces, Chem. Rev. **112**, 5520 (2012).

[5] L. S. O. Johansson, R. I. G. Uhrberg, P. Mártensson, and G. V. Hansson, Surface-state band structure of the $Si(100)2 \times 1$ surface studied with polarization-dependent angle-resolved photoemission on single-domain surfaces, Phys. Rev. B **42**, 1305 (1990).

[6] R. I. G. Uhrberg, E. Landemark, and Y.-C. Chao, High-resolution core-level studies of silicon surfaces, J. Electron Spectrosc. Relat. Phenom. **75**, 197 (1995).

[7] L. S. O. Johansson and B. Reihl, Unoccupied surface-state bands on the single-domain $Si(100)2 \times 1$ Surface, Surf. Sci. **269–270**, 810 (1992).

[8] A. Shavorskiy *et al.*, Sub-nanosecond time-resolved ambient-pressure x-ray photoelectron spectroscopy setup for pulsed and constant wave x-ray light sources, Rev. Sci. Instrum. **85**, 093102 (2014).

[9] S. Neppl *et al.*, Capturing interfacial photoelectrochemical dynamics with picosecond time-resolved x-ray photoelectron spectroscopy, Faraday Discuss. **171**, 219 (2014).

[10] S. Neppl and O. Gessner, Time-resolved x-ray photoelectron spectroscopy techniques for the study of interfacial charge dynamics, J. Electron Spectrosc. Relat. Phenom. **200**, 64 (2015).

[11] T. Arion, S. Neppl, F. Roth, A. Shavorskiy, H. Bluhm, Z. Hussain, O. Gessner, and W. Eberhardt, Site-specific probing of charge transfer dynamics in organic photovoltaics, Appl. Phys. Lett. **106**, 121602 (2015).

[12] See Supplemental Material at http://link.aps.org/supplemental/10.1103/PhysRevLett.132.146201 for 1. Experimental details, 2. SPV shifts for *n*-doped Si(100) with a low charge carrier concentration, and 3. SPV shifts of clean Si(100) for various *p*- and *n*-doped samples measured across microsecond pump-probe delay ranges.

[13] J. P. Long, H. R. Sadeghi, J. C. Rife, and M. N. Kabler, Surface space-charge dynamics and surface recombination on silicon (111) surfaces measured with combined laser and synchrotron radiation, Phys. Rev. Lett. **64**, 1158 (1990).

[14] W. Widdra *et al.*, Time-resolved core level photoemission: Surface photovoltage dynamics of the $SiO_2/Si(100)$ interface, Surf. Sci. **543**, 87 (2003).

[15] M. Weinelt, M. Kutschera, R. Schmidt, C. Orth, T. Fauster, and M. Rohlfing, Electronic structure and electron dynamics at Si(100), Appl. Phys. A **80**, 995 (2005).

[16] D. Bröcker, T. Gießel, and W. Widdra, Charge carrier dynamics at the $SiO_2/Si(100)$ surface: A time-resolved photoemission study with combined laser and synchrotron radiation, Chem. Phys. **299**, 247 (2004).

[17] C. Voelkmann, M. Reichelt, T. Meier, S. W. Koch, and U. Höfer, Five-wave-mixing spectroscopy of ultrafast electron dynamics at a Si(001) surface, Phys. Rev. Lett. **92**, 127405 (2004).

[18] M. Mauerer, I. L. Shumay, W. Berthold, and U. Höfer, Ultrafast carrier dynamics in $Si(111)7 \times 7$ dangling bonds probed by time-resolved second-harmonic generation and two-photon photoemission, Phys. Rev. B **73**, 245305 (2006).

[19] R. Kamrla, A. Trützschler, M. Huth, C.-T. Chiang, F. O. Schumann, and W. Widdra, $SiO_2/Si(001)$ studied by time-resolved valence band photoemission at MHz repetition rates: Linear and nonlinear excitation of surface photovoltage, J. Vac. Sci. Technol. A **37**, 021101 (2019).

[20] W. Eberhardt, G. Kalkoffen, C. Kunz, D. Aspnes, and M. Cardona, Photoemission studies of 2p core levels of pure and heavily doped silicon, Phys. Status Solidi B **88**, 135 (1978).

[21] T. Dittrich and S. Fengler, *Surface Photovoltage Analysis of Photoactive Materials* (World Scientific, Singapore, 2020), ISBN: 978-1-78634-765-7 and references therein.

[22] D. A. Engelbrecht and T. Tiedje, Temperature and intensity dependence of the limiting efficiency of silicon solar cells, IEEE J. Photovoltaics **11**, 73 (2021).

[23] A. Richter, S.W Glunz, F. Werner, J. Schmidt, and A. Cuevas, Improved quantitative description of Auger recombination in crystalline Si, Phys. Rev. B **86**, 165202 (2012).